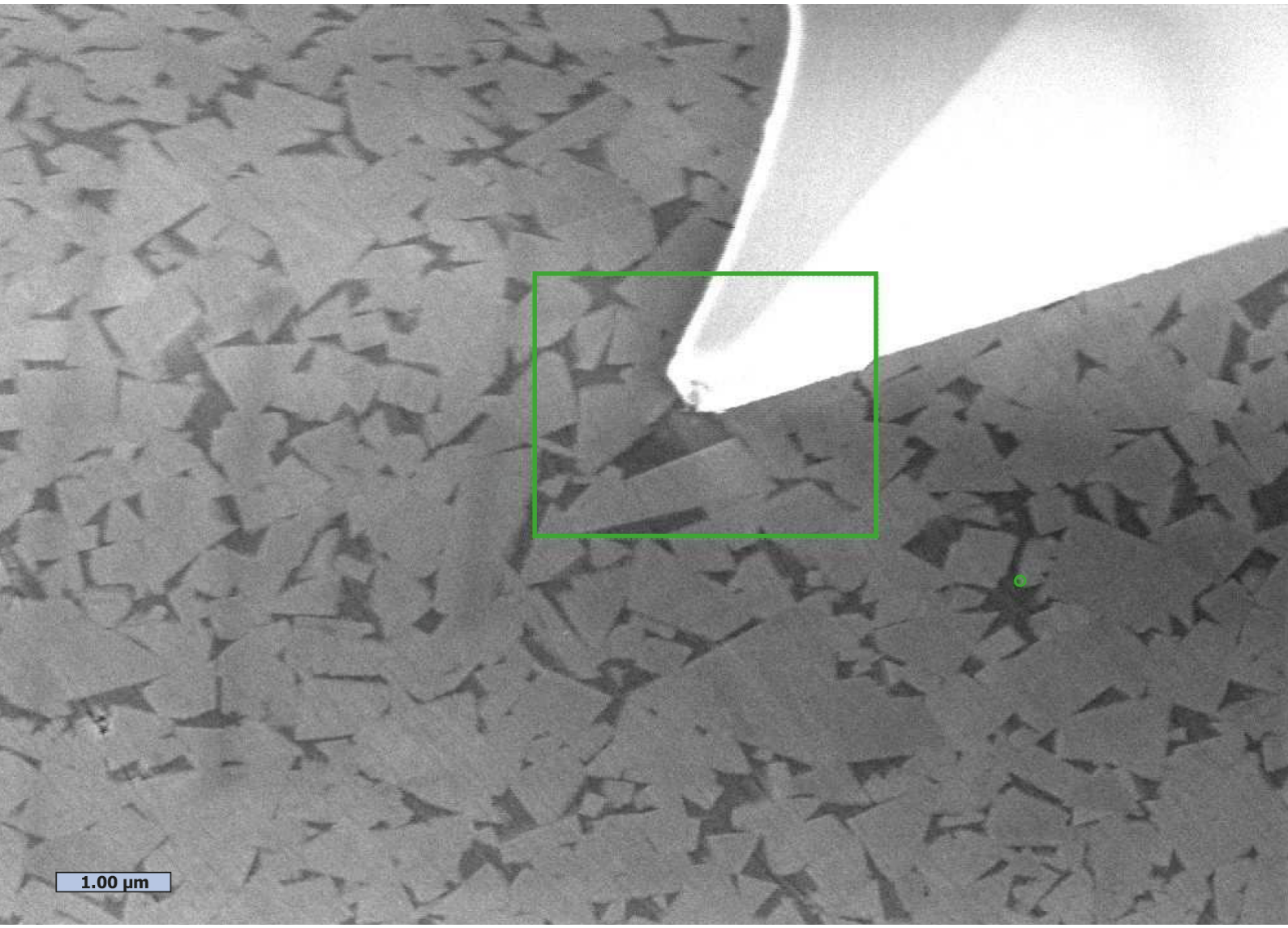

Enabling Scanning Thermal Microscopy in the SEM with an *in situ* AFM

Enabling Scanning Thermal Microscopy in the SEM with an *in situ* AFM

Authors: Frank Hitzel
Semilab Germany GmbH, Germany
Verena Leitgeb
Materials Center Leoben GmbH, Austria
Sabine Lenz
ZEISS Microscopy, Germany

Date: July 2018

Scanning Thermal Microscopy (SThM) performed by an Atomic Force Microscope (AFM) enables thermal characterization of surfaces with lateral resolutions better than 50 nm. An additional capability of SThM, besides this mapping the temperature distribution, is the ability to image the local thermal conductivity. Thermal microscopy has been implemented in the ZEISS Integrated Atomic Force Microscope, the solution for true *in situ* measurements for ZEISS FE-SEMs and FIB-SEMs now for the first time. It enables measurements of temperature related parameters inside an SEM under vacuum conditions. This leads not only to higher resolution of temperature maps than under ambient conditions, but also enables investigations of *in situ* temperature changes caused by an electron beam, and potentially an ion beam, as well as making navigation to the area of interest easier. This report describes the first experiments performed with the newly created SThM-setup.

Introduction

A key point when designing highly integrated devices nowadays is heat generation and heat transport. Active components such as CPUs and LEDs dissipate energy up to several 100 W per cm^2.

Without careful design of the heat transport paths, such devices would die within a few milliseconds. Knowledge of heat distribution and thermal conductivity in the nanometer scale helps to find the right strategy for energy transport, in particular when designing new devices.

The AFM is the only instrument that enables measurement of local heat distributions with high lateral resolution below 50 nm. For this purpose, there are special AFM tips that have, for example, a resistor for temperature measurements directly at the tip. While the AFM tip is scanned over the surface, the tip simultaneously records the topography of the sample via its mechanical bending and the temperature via measurement of the resistance value. By applying higher currents to the AFM tip, it also acts as a heating device enabling measurement of the heat transport away from the tip and giving information about local thermal conductivity. The thermal conductivity information obtained in this way can even be quantitative, as demonstrated by Fiege et al. [1].

Experimental Setup

The basis for the experiments is ZEISS Integrated Atomic Force Microscope. This is an *in situ* AFM for integration into a SEM operating with beam deflection technique and enabling the use of all standard AFM cantilevers (Fig. 1).

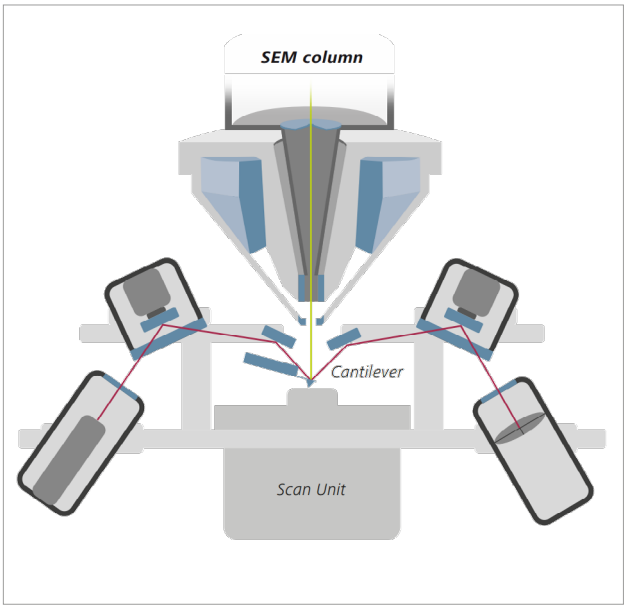

Figure 1: *AFM Option Schema*

For this work, the system was operated in a FE-SEM, ZEISS Merlin, having a Gemini 2 column with continuous beam current.

In order to enable SThM in the SEM-AFM, a new cantilever holder has been designed, which is compatible for holding SThM tips from the manufacturer Kelvin Nanotechnology. These tips are made of silicon with two gold areas at the back side of the cantilever, which are connected to the resistive element on the tip (Fig. 2).

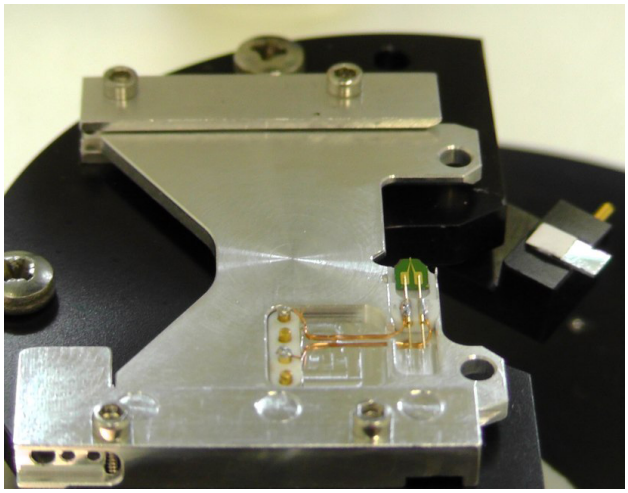

Figure 2: *Cantilever holder for SThM*

In contrast to the normal cantilever holders with only one pin, this newly designed holder uses two gold pins which are pressing down on the gold electrodes of the cantilever body. Via two shielded 50 Ω cables, the signals are then accessible at the exterior side of the connector box of the AFM. The system design enables the cantilever to be mounted and electrically checked outside the vacuum and then using the SEM airlock to transfer the connected tip into the system.

The tested AFM tips have a temperature sensitivity of about 1 Ω/°C. The tip is connected via a resistor bridge in order to eliminate the resistive offset to be able to sufficiently increase the gain enough (Fig. 3). The bridge resistors R1 are matched to the tip resistance of about 300 Ω. The input power for the bridge is applied as an AC signal from an AC output of the AFM controller. The bridge output is amplified by approximately 100 times and then fed back into one of the inputs of the AFM controller. The measurement signal is then generated by one of the integrated lock-in channels.

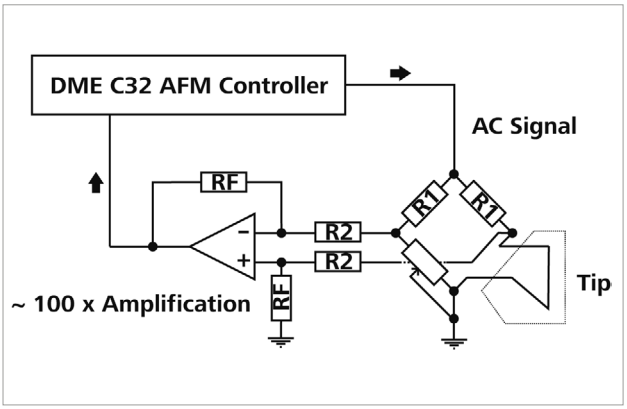

Figure 3: *Electrical Connection Diagram*

Theory

When applying an AC signal with the frequency ω to the resistive tip, according to [1], the temperature of the tip oscillates with the amplitude

$$\Delta T = \frac{P}{\pi\, k}\,(C - \ln(\omega)) \qquad \textbf{[1]}$$

Here P is the amplitude of the power per unit length, *k* is the thermal conductivity and *C* is a constant. As expected, a higher thermal conductivity leads to a lower temperature oscillation at the tip.

The tip resistance depends approximately linearly on the tip temperature. With the resistor bridge the change of the voltage drop over the tip is measured. According to [1], the voltage is given by:

$$\begin{aligned} U(t) \;=\; & R_{dc}\, I_0 \sin(\omega\, t) \\ & + I_0 \frac{dR}{dT}\frac{\Delta T}{4}\sin(\omega\, t - \phi) \\ & - I_0 \frac{dR}{dT}\frac{\Delta T}{4}\sin(3\,\omega\, t - \phi) \end{aligned} \qquad \textbf{[2]}$$

Here, I_0 is the electrical current amplitude and *dR/dT* the temperature coefficient of the tip. When applying an AC signal with the frequency ω, the heating power and therefore also the temperature and the resistance oscillate with 2 ω. As the current still oscillates with the base frequency, there are in fact two frequencies ω and 3 ω in the measurement signal. The 3 ω component is independent of the base resistance R_{dc}, which itself depends on the actual temperature of the tip, i.e. the 3 ω signal is independent of the tip temperature. If the 3 ω signal is measured at two different frequencies, it is possible to calibrate the remaining propor-

tionality factors with a known material and directly measure the thermal conductivity *k*. At a single frequency, relative changes of the thermal conductivity can still be achieved.

Measurements

Fig. 4 shows an SEM image of the tip inserted in the AFM. The reflective area with the two conductors protruding to the tip can clearly be seen. The size of the reflective area used for the AFM force measurement is comparable to that of a normal AFM cantilever.

Fig. 5 shows an image of the tip as it is being moved towards the surface. It shows that the contact area is relatively small in comparison to the dimensions of the tip end with its resistive element.

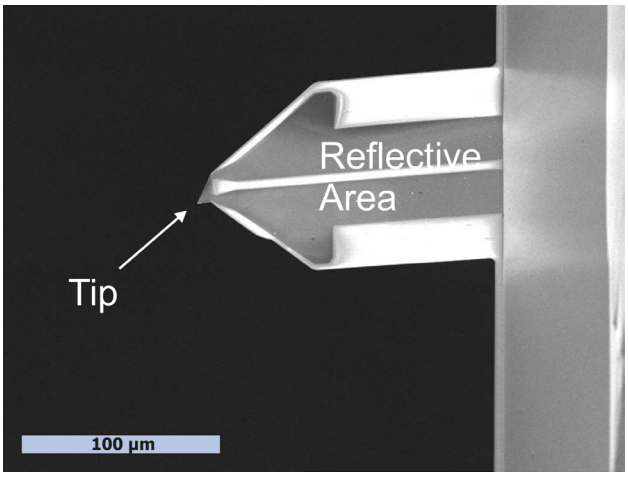

Figure 4: *Tip Dimensions*

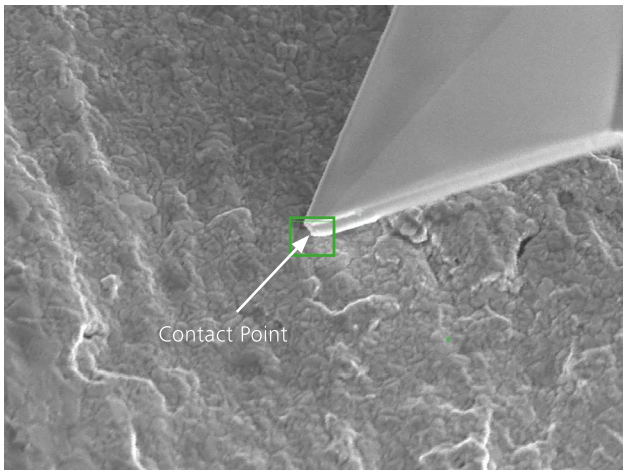

Figure 5: *Tip approached on a copper surface*

After applying a 300 mV AC signal with 100 Hz frequency to the bridge and compensating the bridge for minimal output, one can clearly see the two frequencies at 100 Hz and 300 Hz in the screen shot shown in Fig. 6. The peak heights can directly be measured by using the lock-in amplifiers in the C32 AFM controller. The first question to arise was how much the temperature amplitude varies between tip at the sample and tip away from the sample state (compare Table 1).

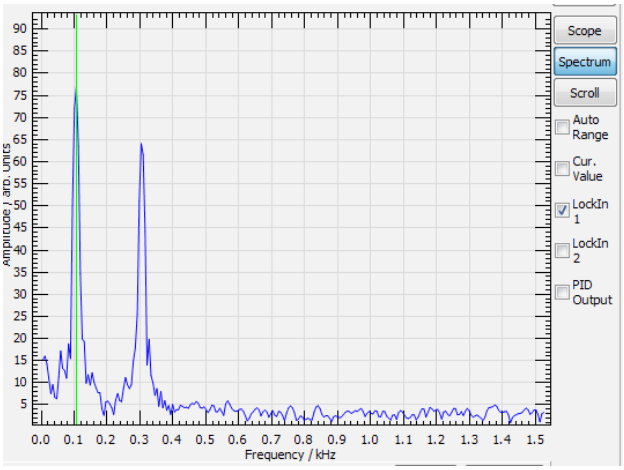

Figure 6: *Frequency Spectrum as shown in the software during operation*

Tip Position	Output
Away from Surface	7.69 V
At the Surface	7.78 V

Table 1: *Lock-in output at 3 ω component. At 300 mV on the bridge, the voltage drop on the tip was 150 mV. The Lock-In gain was set to x1024 for this measurement.*

For a copper film sample, the obtained amplitude change of the 3 ω signal was about 93 mV, as shown in table 1. As the lock-in gain was set to about x1024 and the bridge amplifier gain was 100, this corresponds to an oscillation amplitude of 9.3 µV. So the factor of the last term in equation [2] becomes:

$$I_0 \frac{dR}{dT} \frac{\Delta T}{4} = 9.3\,\mu\mathrm{V} \qquad [3]$$

Assuming a resistance of about 300 Ω for the tip, the base current amplitude I_0 can be calculated to 0.5 mA. Replacing *dR/dT* with 1 Ω/°C and I_0 with 0.5 mA, results:

$$\Delta T = 74\,\mathrm{mK} \qquad [4]$$

This is the magnitude of the temperature oscillation at the tip caused by the applied AC voltage.

Beam Position	Output
On the tip (lower third)	1.9 V
On the sample close to the tip	0.9 V
Off	1.5 V

Table 2: *Lock-in output at 1 ω component. Again 300 mV on the bridge and Lock-In gain x 1024*

Influence of the Electron Beam

In order to investigate the temperature change of the tip due to the electron beam, the lock-in was set to the 1 ω reference frequency and the SEM was switched to spot mode. The electron beam was set to 5 kV at a beam current of 1 nA.

It was found that the detected heating on the tip caused by the electron beam was highest in the lower third of the tip triangle, while no heating was observed when the electron beam was focused on the sample, even getting very close (100 nm) to the tip (see table 2). The lock-in was still running with x1024 gain. The voltage difference is one order of magnitude higher than in the experiment before. But in this case the change of the tip resistance R_{DC} was caused by the electron beam that generates the signal (see Table 2).

Relating the applied voltage of 150 mV on the tip to the measured voltage with the lock-in, the resistance change of the tip can be calculated back to:

$$\frac{0.01\,\mathrm{mV}}{150\,\mathrm{mV}} \cdot 300\,\Omega = 0.02\,\Omega \qquad \textbf{[5]}$$

Assuming again 1 K/Ω temperature dependence of the tip, this corresponds to a temperature change of 20 mK caused by the electron beam.

To give an estimation of the signal-to-noise ratio of the temperature change caused by the electron beam, Fig. 7 shows a screenshot of the interactive measurement dialog in the AFM software. Here the heating of the electron beam can clearly be seen by a signal jump from about 0.9 V to 1.9 V. As expected, the 3 ω signal is not influenced by the tip temperature, therefore here no influence of the electron beam could be measured.

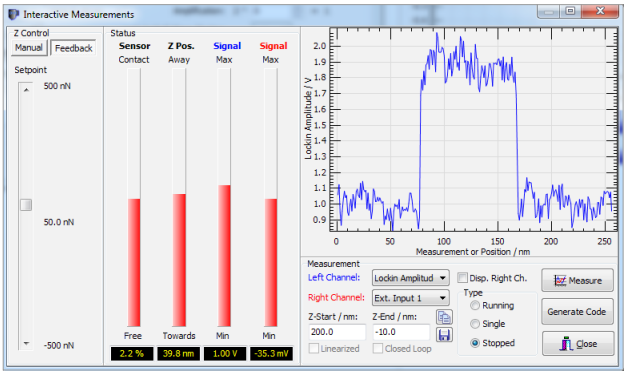

Figure 7: *Signal Pulse on Lock-In output caused by the electron beam*

Influence of the AFM Laser

In vacuum it is likely that the AFM laser warms up the AFM tip to some extent. It was possible to verify this. At an applied voltage of 50 mV on the bridge, the lock-in output varied by 100 mV between laser on and off. Using the same calculation as above, the following is obtained:

$$\frac{0.001\,\mathrm{mV}}{50\,\mathrm{mV}} \cdot 300\,\Omega = 0.006\,\Omega \qquad \textbf{[6]}$$

There was a temperature change of 6 mK at the tip caused by the beam detected on the cantilever back side.

To further evaluate this, it could be compared with a known heating caused by the electron beam when the beam is moved from the tip end to the reflective area. However, this is yet to be tried.

Temperature Sensitivity

In order to obtain quantitative values of the tip sensitivity, a miniature hotplate with a size of approximately 1 × 1 mm was used, which was manufactured by the company ams AG in Austria. An image of the hotplate is shown in Fig. 8. It is a lithographically made chip with a resistive heating area in its center. For isolation from the bottom, the center part of the structure is undercut. The temperature can be obtained by evaluating the resistivity of the structure. The contacts H1 and H2 were used for applying the heat current. The connection between the chip and electrical pins on the chip holder was established by drawing two lines with conductive silver paste and two thin copper wires.

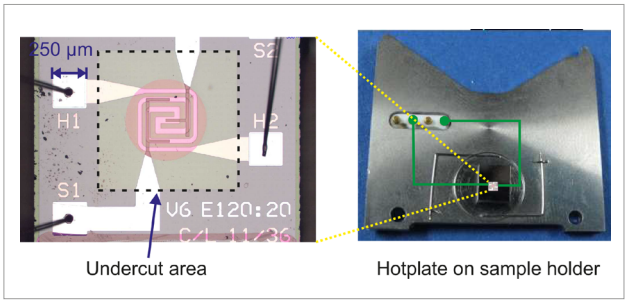

Figure 8: *Miniature hotplate for checking tip sensitivity*

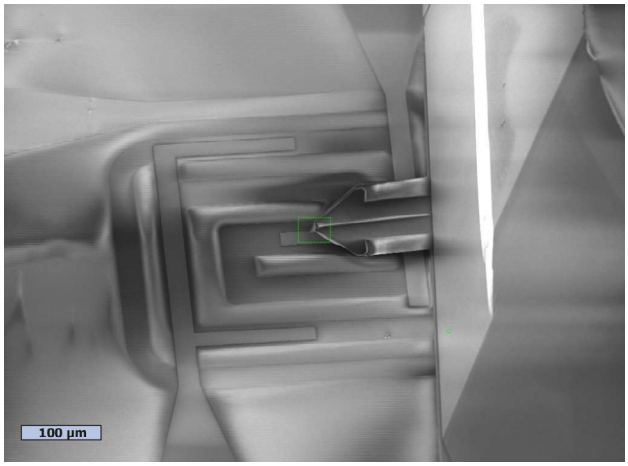

Figure 9: *SThM tip approached on hotplate*

The hotplate was approached by the tip approximately in the center (see Fig. 9) and several positions in this area were tried without significant differences. Table 3 shows the lock-in output voltage for the 1 ω signal while the hotplate was heated to about 215 °C. In this setup, the lock-in gain was set to 512, and the applied voltage at the tip was again 150 mV. A resistivity change of the tip was obtained:

$$\frac{17\mu\mathrm{V}}{150\mathrm{mV}} \cdot 300\,\Omega = 0.035\,\Omega \qquad \textbf{[6]}$$

Tip Position	Output/V
Far away from surface	3.5
10 m away from surface	3.7
on the surface	4.4

Table 3: *Output voltage for tip on heated hot plate while hot plate at about 215 °C*

The 215 °C temperature on the hotplate changes the tip temperature by only 35 mK. This shows the heat flow to the cantilever body is in vacuum some orders of magnitude larger than the heat flow coming from the sample surface. The noise level on the lock-in output in this state is at about 20 mV, enabling the measurement of the sample temperature in vacuum with an accuracy of about 4 K.

For comparison, the same experiment was performed under ambient conditions. The hot-plate was heated to a value around 150°C, with a voltage of 150 mV applied to the tip. This resulted in a change of voltage in the lock-in output of 1.5 V while the lock-in gain was at a value of only 128. For the resistivity change, the following is obtained:

$$\frac{117\mu\mathrm{V}}{150\mathrm{mV}} \cdot 300\,\Omega = 0.23\Omega \qquad \textbf{[7]}$$

Scanning Thermal Images

The most important field of application of an SThM tip is to generate images of thermal conductivity and temperature. For testing SThM for thermal conductivity, a tungsten carbide sample has been investigated, where tungsten-carbide grains are immersed in a cobalt matrix, which can be clearly distinguished by SEM. The corresponding SEM image is shown in Fig. 10. The tungsten-carbide crystals appear as triangular and rectangular brighter crystals inside a darker cobalt matrix. The corresponding SThM images are given in Fig. 11. The image position corresponds approximately to the green marked area in Fig. 10. In the AFM topography, the tungsten-carbide crystals can be clearly identified. Comparing the topography and the thermal conductivity images, there is a correlation but not a 100 % match. The conductivity image is shifted by some 100 nm to the lower right, meaning that the topography creating tip part is not exactly at the same location as that part being most sensitive for thermal conductivity. Some of the crystals seem to appear stronger in the conductivity image than in the topography image.

The surface of the sample shows polishing groves with a depth of about 1-2 nm which run from the upper left to the lower right corner. These stripes are also clearly visible in the conductivity image. As the surface topography strongly influences the contact area between tip and sample, this was to be expected.

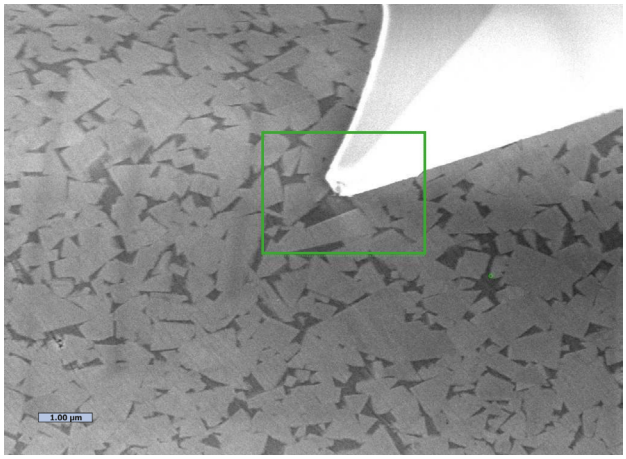

Figure 10: *SThM tip approached on tungsten carbide sample*

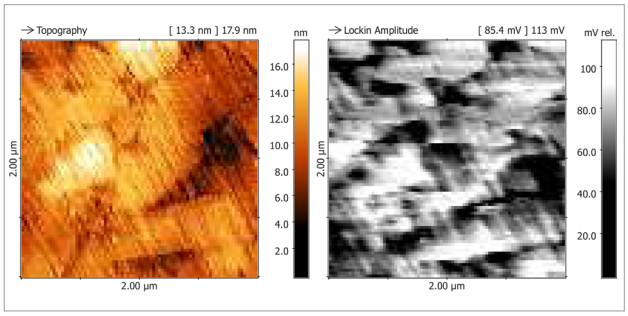

Figure 11: *SThM 3 ω measurement on tungsten carbide, left: topography, right: thermal conductivity*

A structured gold sample, which gives no material contrast has been used in order to investigate the topography dependence. A profile measurement of this sample is given in Fig. 12. The blue profile line shows the scan over a step on the surface. The green line resembles the lock-in output at the 3 ω frequency. It can clearly be seen that the lock-in output is decreased directly at the step. The jump in the green line corresponds to an output voltage change of about 50 mV at 8 V full signal output. The lower output signal of the lock-in corresponds to a smaller temperature variation and therefore a higher thermal conductivity. I.e. the thermal conductivity is increased at the edge. The possible reason for this could be a larger contact area when the tip is directly at the edge.

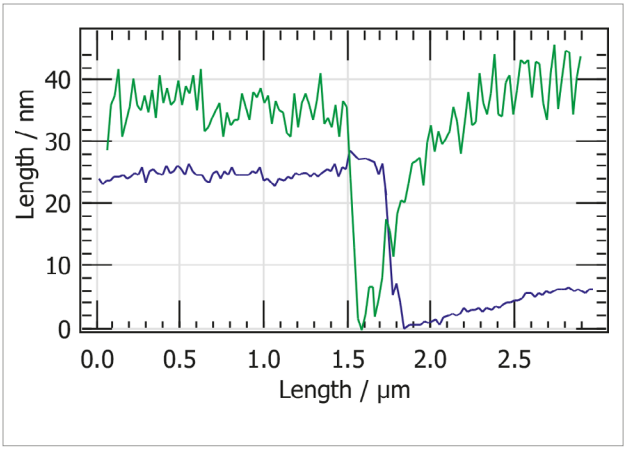

Figure 12: *Prole measurement on a structurized gold sample. The blue line indicates the topography, the green line the thermal conductivity.*

Summary

The necessary functionality to perform SthM in the scanning electron microscope has been created, consisting of a specially designed sample holder for connecting the two pins of a resistive probe and a resistor bridge amplifier. The capability to measure sample temperature and thermal conductivity in vacuum has been demonstrated. These are contained in the base and frequency tripled signal, respectively, of an applied AC voltage.

It was found that the thermal interaction between tip and sample is about a factor of 10 weaker in vacuum than in air. Furthermore, it was shown that the temperature which is represented by the 1 ω signal of the thermal tip is influenced by both the electron beam as well as the AFM laser, while the 3 ω signal is independent of the tip temperature and therefore not influenced by SEM beam and AFM laser. Finally, the scanning capability of the thermal probe on a tungsten carbide sample was demonstrated, clearly revealing the crystal structure also in the thermal conductivity image. On an unstructured gold sample, it was shown that the measured thermal conductivity is in fact influenced by the surface topography, where a surface step induced an increase of the measured thermal conductivity.

References:

[1] G. B. M. Fiege, A. Altes, R. Heiderhoff, and L. J. Balk. Quantitative thermal conductivity measurements with nanometre resolution. J. Phys. D: Appl. Phys, 32(5): L13-L17, March 1999.

Carl Zeiss Microscopy GmbH
07745 Jena, Germany
microscopy@zeiss.com
www.zeiss.com/microscopy